Research Note

Three Dimensional Numerical Modelling of Stone Column to Mitigate Liquefaction Potential of Sands

Morteza Esmaeili[1] and Seyed Mehrab Hakimpour[2]*

1. Assistant Professor, Department of Railway Engineering, Science and Technology University, Tehran, Iran, * Corresponding Author; email: m_esmaeili@iust.ac.ir
2. M.Sc. Graduate, Department of Railway Engineering, Science and Technology University, Tehran, Iran

ABSTRACT

Liquefaction is one of the most essential causes of failure of transportation infrastructures, especially the road and railroad based on saturated fine sand substrates under seismic conditions. Meanwhile, applying stone columns in a group form is considered as a method to control this phenomenon. To do so, Model No (1) of VELACS project, including NEVADA sand with relative density of %40, was first evaluated numerically using FLAC3D, in which finite difference and sufficiency of Finn constitutive model in liquefaction simulation was shown. Then, sensitivity analysis was performed to examine its radius and depth of influence on reducing excess pore water pressure by imposing a stone column in the center of the model and changing its diameter. In the final step, sensitivity analysis was performed on their efficiency to control liquefaction by simulating the group stone column with square layout and changing diameter of columns and their center-to-center distance. The results of numerical analyses show that the performance of the single stone column increases in reducing excess pore water pressure by increasing depth. Generally, it can be stated that at the depth of 1.25 m and 2.5 m the effective area of the column is 3 and 4 times bigger than the stone column diameter. Columns distance proportion to stone columns diameter (s/d= 2, 3, 4, 5) was evaluated for the group stage. Moreover, the single manner in the group forms more effective than a single column. The group performance of columns appeared to be better than the singular ones.

1. Introduction

Liquefaction is a phenomenon that is responsible for major damages and great losses in historical earthquakes around the world. The risk of liquefaction and related ground deformation can be reduced by various ground improvement methods, including densification, solidification (e.g., cementation), vibro-compaction, drainage, explosive compaction, deep soil mixing, deep dynamic compaction, permeation grouting, jet grouting, pile-pinning and gravel drains or stone column [1]. A well-known method,

the stone column method is discussed in this paper. In this regard, among the stabilization methods, using the stone column, in which a part of bed's loose material is replaced with crushed stone materials, is considered as a cost-effective and environment-friendly solution. Loose soil rehabilitation using this method is generally identified by two approaches; increasing bearing capacity by increasing soil's shear strength, and controlling settlement. This paper proposes the use of numerical simulations to

evaluate radial drainage and excess pore pressure in the presence of an improvement method. This paper includes numerical simulation of centrifuge experiments aiming at identifying key considerations for the use of stone columns as a ground stabilization measure against seismic-liquefaction. For this purpose, first, the liquefaction potential of sandy beds without the presence of stone columns was investigated by using the finite difference computer code FLAC3D. The result of developed model was validated on the basis of centrifuge test results from the well-known VELACS experimental project [2]. In particular, model test No. 1 was used to simulate the three-dimensional (3D) response of the liquefiable soil layer. Then, using the validated numerical model, a single column with different diameters as well as group columns with different diameters and distances were simulated, and the effect of single stone columns and group per-formances and their efficiency domain were investigated in liquefaction mitigation.

2. Literature Review

The effectiveness of stone columns in mitigating liquefaction is reported in earthquakes case histories and limited centrifuge tests (e.g., [3-4]). The men-tioned works comprises of two main categories as numerical analysis and laboratory experiments. Experimental project Include, Brennan [5], which investigated the effects of vertical drainage system on the liquefaction control in sandy materials by centrifuge test, and Adalier [4] studied the stone columns through centrifuge tests for the case of the liquefaction countermeasure in non-plastic silty soils. Besides, Brennan and Madabhushi [6] studied the liquefaction remediation by vertical drains with varying penetration depths through centrifuge test. The numerical studies were done

by Olgun and Martin [7], and Rayamajhi et al. [1] based on two or three dimensional analysis with single columns. Others, for instance Bouckovalas [8] and Papadimitriou et al. [9], drew a comparison between 1D and 2D analyses. Besides, Asgari et al. [10] run the numerical simulation of improvement for a liquefiable soil layer using stone column and pile-pinning techniques. Brennan et al. [11] modeled the effect of gravel drainages in liquefaction mitigation in sandy soils using 2D finite difference method.

3. Numerical Model of the Centrifuge Test

The case selected for this analysis is the centrifuge experiment No. 1 conducted during the course of the VELACS project by Arulanandan [2].

3.1. Model Geometry, Motion Characteristics and Boundary Conditions

Figure (1) shows the arrangement of the horizontally layered loose sand in a laminar box for Model test No. 1. The laminar box consisted of a 20 cm high, horizontal layer of uniform Nevada No. 120 sand, placed at a relative density of 40% by dry eluviation. It was fully saturated with water, spun at a centrifuge acceleration of 50 g, and excited horizontally at the base. This combination was to simulate a 10 m soil layer in prototype. The input horizontal acceleration time history at the base of the box consisted of 20 cycles of a 100 Hz sinusoidal input, with variable amplitude and maximum peak acceleration of 11.75 g. For the 50 g centrifuge acceleration of the test, this corresponds to a frequency of 2 Hz and peak acceleration of 0.235 g in the prototype, and a zero vertical acceleration was considered [2]. Some of the material para-meters are extracted from Arulmoli et al. [12], and
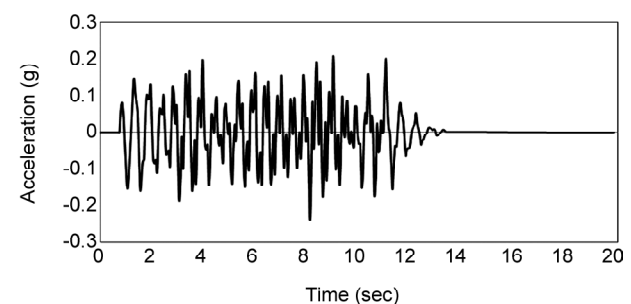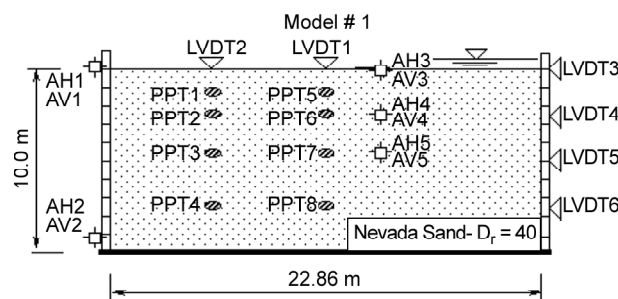

Figure 1. Cross-sectional view of the centrifuge experiment No.1 and horizontal input motion at bottom [2].

characteristics of Nevada sand, soil with 40% density is given in Table (1).

The soil was modelled with continuum zones. Figure (2) shows the finite-difference grid used in the FLAC model for the soil. The foundation was assumed to be rigid. When subjected to base shaking, the soil in the laminar box simulates approximately a semi-infinite layer. In order to reflect the semi-infinite condition in the numerical model, the grid points at the same horizontal level are tied-up together. In other words, the grid points at the same level are allowed to be displaced by the same amount. In regard to the dimensions of VELACS experiment [12] model No. 1 and considering the scale factor of 1 to 50 in the centrifuge experiment, the numerical model geometry was considered with a depth of 10 m and the model's dimensions at X directions were considered equal to 22 m and at Y directions equal to 16 m. For centrifuge test modelling, the boundary conditions were closed on four sides, and at the bottom a hard bed was considered.

3.2. Constitutive Model for Liquefaction

In the present analysis, Mohr-Coulomb plasticity model has been used for the NEVADA sand. Dynamic pore-pressure generation can be modelled by accounting for the irreversible volume strain in the constitutive model. This is done with the modified form of the standard Mohr-Coulomb plasticity model called "Finn Model" [14] that is incorporated in FLAC3D, which can perform coupled dynamic-groundwater flow calculations and can simulate the effects such as liquefaction. Byrne [15] proposed Eq. (1) to numerical modelling of liquefaction, where: the increment of volume decrease, to the cyclic shear-strain amplitude, γ:

$$\frac{\Delta\varepsilon_{vd}}{\gamma} = C_1 \exp(-C_2(\frac{\varepsilon_{vd}}{\gamma})) \qquad (1)$$

3.3. Wave Transmission and Mechanical Damping Model

The finite difference grid dimensions were selected by taking into account the maximum frequency of the shear wave that the model could logically respond to during earthquake loading. The lowest shear wave velocity in the model belongs to the soil deposits, the highest admissible frequency for a propagating shear wave is 4 Hz. Therefore, the input earthquake record shall be filtered by a low pass filter to remove frequency components higher than 4 Hz. Then, uniform zone size of 1 m x 1 m was selected. Local damping is originally designed as a means to equilibrate static simulations. It can be expressed by Eq. (2) [13]:

$$\alpha_L = \pi \cdot D \qquad (2)$$

where α_L is the local damping coefficient, and D

Table 1. The characteristics of Nevada sand, soil with 40% density [12].

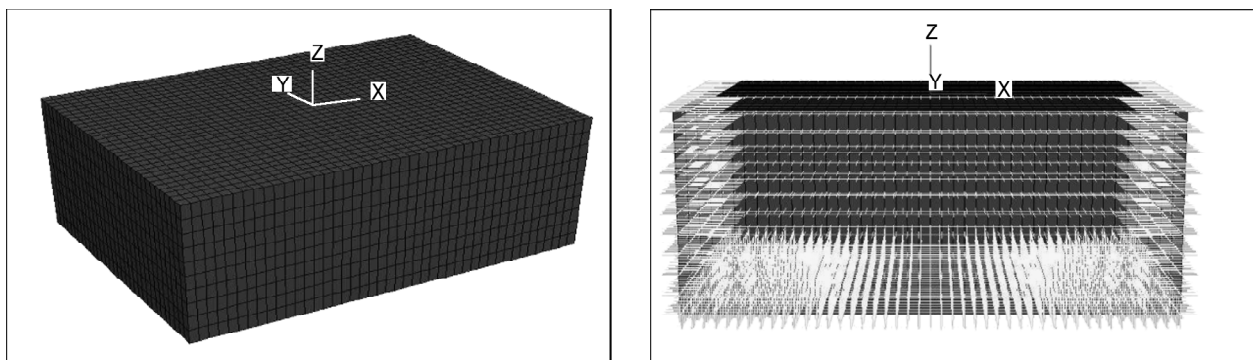| Characteristics	Cohesion	Permeability	N-SPT	Friction Angle	Shear Modulus	Dry Density	Poisson's Ratio	Porosity
Unit	kPa	m/s	Blows	Degree	MPa	Kg/m^3	-	-
Values	0	6 x 10^{-5}	7	30	3.85	1500	0.3	0.42

Figure 2. Finite difference model of soil and centrifuge laminar box [13].

is the critical damping and equals 0.05. Local damping appears to give good results for a simple case because it is frequency-independent and needs no estimate of the natural frequency of the system being modelled. A local damping equal to 0.157 was used to simulate soil liquefaction in this paper.

3.4. Analysis Approach

3.4.1. Static Analysis

The initial geostatic stress for steady state in a free field is one of the primary values related to grid zones, which forces the model to reach equilibrium by performing mechanical calculations. In the static analysis, the soil was under gravity loading only; the base boundary was fixed in all directions and the side boundaries were fixed in the x and y direction. A static equilibrium calculation always precedes a dynamic analysis.

3.4.2. 3D Dynamic Analysis

As the VELACS loading chamber has a limited dimensions in plan, some 3D problems will arise during the seismic excitation because of boundary effects. In this regard and due to the 3D nature of liquefaction and stone columns in the next step, basically, a 3D numerical model development was essential in the present study. It could be claimed that the complexity of the presented numerical model leads to more precise results in comparison to 2D plain strain model. The dynamic loading in this simulation is applied as acceleration time history at the bottom of the model with 2 Hz frequency and 0.235 g acceleration. Dynamic analyses were performed and the results were extracted for interpretation and further assessment [2].

3.5. Validation of a Numerical Model

Figure (3) to (6) displays the results of numerical modelling and the centrifuge experiment No. 1 in the VELACS project [2] in the terms of excess pore water pressure at depths of 1.25 m, 2.5 m, 5 m, and 7.5 m. Very good agreement is achieved between the numerical results and experimental responses. Pore water pressure rises throughout the soil layer during the shaking and reaches to the initial effective vertical stress level in the upper layers, which is
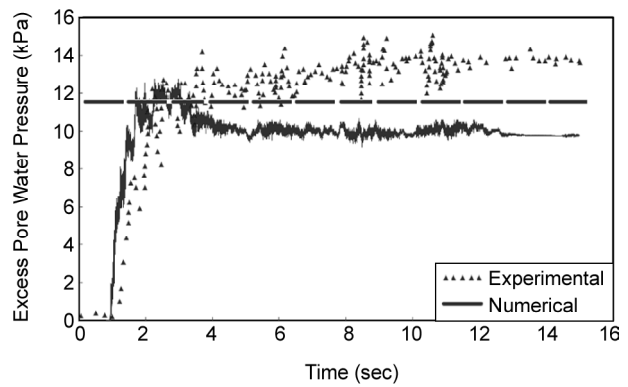

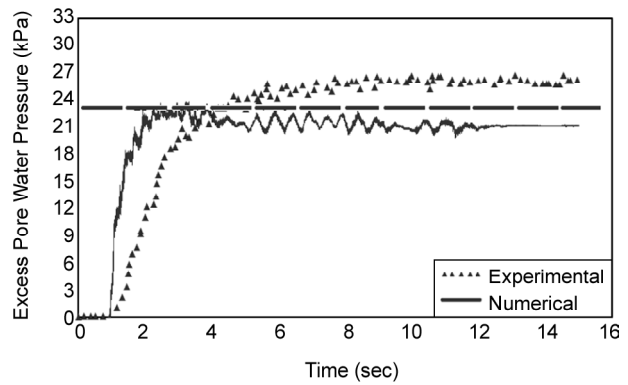**Figure 3.** The excess pore water pressure at depth of 1.25 m.

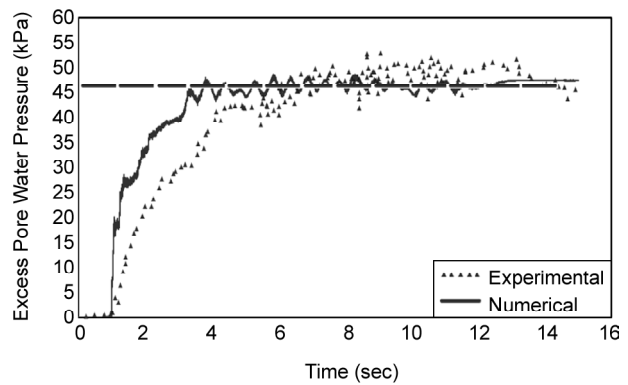**Figure 4.** The excess pore water pressure at depth of 2.5 m.

Figure 5. The excess pore water pressure at depth of 5 m.
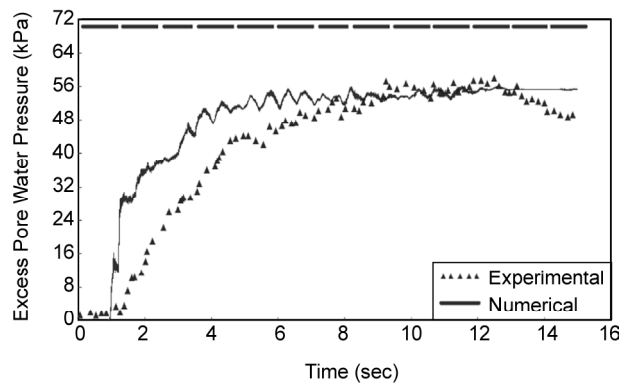

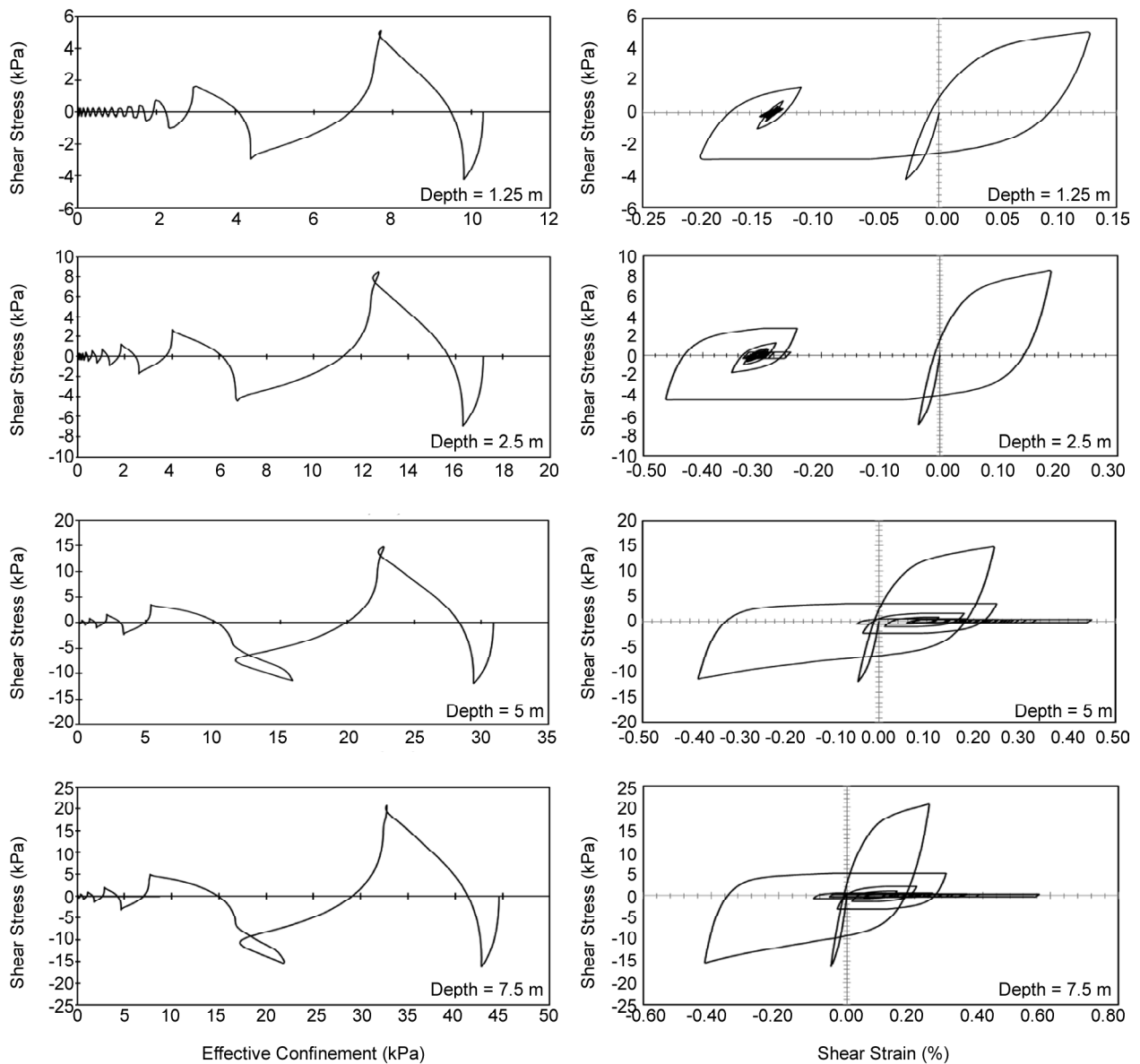**Figure 6.** The excess pore water pressure at depth of 7.5 m.

Figure 7. Computed shear stress-strain and effective stress paths at different depths in the numerical modelling.

associated with producing a state of liquefaction. In these results, the range of zero effective stress is signified by a horizontal line in the diagram. However, in reality, the pore pressure starts to dissipate after a few seconds elapsed in sands as they have high permeability.

The stress-paths of Figure (7) show the typical mechanism of cyclic decrease in effective stress due to pore pressure build up. The numerical modeling of result for saturated loose cohesionless soils (NEVADA sand with relative density of %40) the presented dynamic excitation response shows minor cyclic mobility effect under level ground conditions.

Figure (8) shows the recorded and predicted

acceleration at the depth of 0, 2.5 and 5 meters by the accelerometers AH3, AH4 and AH5, Figure (1). It is evident that the model predictions closely agree with recorded acceleration with depth increases. Thereafter, the predicted accelerations ttenuate very rapidly because the assumption of undrained condition makes the sand layer liquefy sooner than for the actual case.

Besides, the results show that the initial liquefaction occurs sooner in the numerical modelling than in the centrifuge test. It can be because using the base boundary and side boundaries are completely impermeable and turn off the flow calculation option in the dynamic analysis. It's worthy to mention that neglecting the effective stress analysis
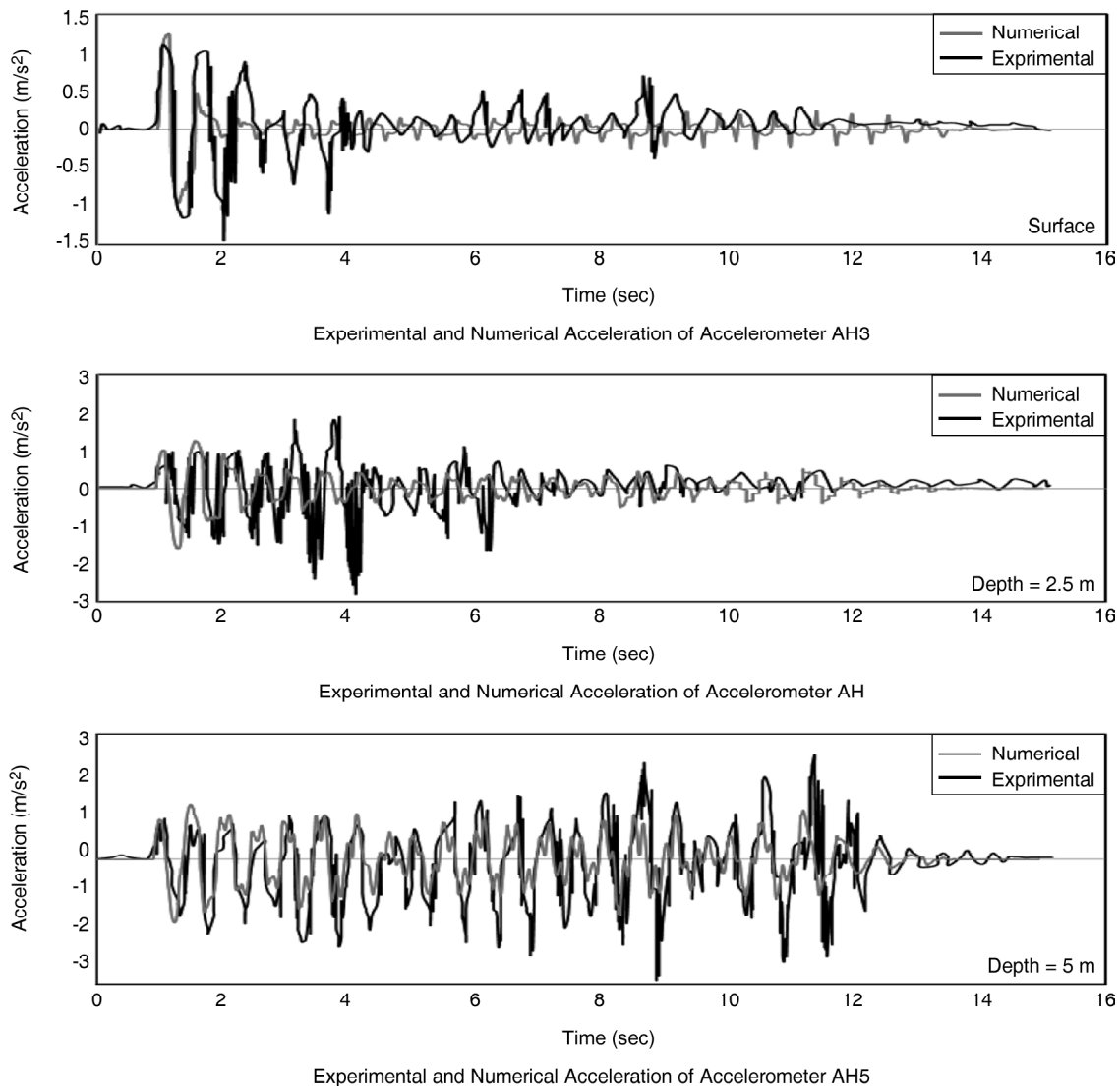
Figure 8. Experimental and numerical acceleration.

in modeling doesn't impair the role of excess pore pressure water.

4. Numerical Modelling of Single Stone Column

In this section, in order to determine the efficiency of stone column in decreasing pore water pressure of the surrounding soil, the dynamic analysis was performed by considering a column in the center of the VELACS model No. 1 [2] with 90, 120 and 150 cm diameters, thus the excess pore water pressure was investigated at different distances from the stone column. To assimilate the single stone column, boundary conditions, wave transmission and input motion in the numerical model VELACS model No. 1 [2] were used. Mohr-Coulomb model defined for stone column material and Finn model was used for liquefaction simulation of NEVADA

sand.

4.1. Seismic Shear Stress Redistribution

Baez and Martin [16] introduced the concept of seismic shear stress redistribution due to Vibro stone columns. Since the Vibro stone columns are stiffer than the soil being treated, it was thought the earthquake-induced shear stress would mostly be concentrated in stone columns, leading a reduction in shear stress in the soil medium. Baez and Martin [16] reported values between 2 and 7 for stone columns, whereas larger values can be expected for soil-cement columns. The assumption of shear strain compatible deformation of discrete columns and surrounding soil always leads to a reduction in the computed dynamic shear stress in the surrounding soil for all combinations of $Ar > 0$ and $G_r > 1$. Hence

the reduction in shear stress is a function of the shear modulus ratio. The formula proposed by Baez and Martin is an Eq. (3):

$$G_r = \frac{G_{SC}}{G_S} \qquad (3)$$

where G_{SC} and G_S are shear moduli of stone column and soil being treated, respectively. This ratio is a critical parameter for stress concentration or stiffening effects due to the introduction of a stone column system, and in this study, for achieving the maximum stiffening, $G_r = 6$ was applied.

4.2. Model Geometry

The stone columns were modelled using cylindrical meshes and were assumed to have the Mohr-Coulomb constitutive behavior. The properties of the stone column material used in the analysis are tabulated in Table (2). In general, the ATTACH command provided by FLAC 3D was used to join the grids on different segments. However, since wedges mesh was used in the soil section, the use of the cylindrical mesh for the stone column created a problem with mesh disparity for direct use of the ATTACH command. Therefore, an interface was used to join the two grids in the soil section.

4.3. Soil-Stone Column Interface

The interfaces between the stone column and surrounding soil were modelled as linear spring-slider systems, with interface shear strength defined by the Mohr-Coulomb failure criterion. The relative interface movement is controlled by interface stiffness values in the normal k_n and the tangential k_s directions. Based on the recommended rule-of-thumb estimates for maximum interface stiffness

values given by Itasca consulting group, k_n and k_s were set to ten times of the equivalent stiffness of the neighboring zone according to Eq. (4) [13]:

$$k_s = k_n = \max \left[10 \times \left[\frac{K + \frac{4}{3} G}{\Delta z_{min}} \right] \right] \qquad (4)$$

where K and G are the bulk and shear modulus of soil zone, respectively, and is the smallest dimension of an adjoining zone in the normal direction. Table (3) summarizes the interface stiffness properties used in the simulations after adjustment of values calculated by using Eq. (4)

4.4. Numerical Results of Single Stone Column

The lateral boundary conditions were closed on four sides, and at the bottom a hard bed was considered as imposed by the laminar box device in the centrifuge test. VELACS input motion was applied at the bottom of the model after filtering out the high frequency components of the recorded motion. During the dynamic loading, the pore water pressure was investigated at different distances from the stone column. The dynamic analysis results for 1.25 m depth of 1 m, 1.5 m, 2 m, and 2.5 m distances from the column's center are shown in Figures (9) to (12). Besides, the effective stress is equal to 11.5 kPa (red line) corresponding to static conditions in depth of 1.25 m.

Tables (4) and (5) show the results of numerical modelling of the single stone column for a depth of 1.25 m. The results show that the circular region around the column is affected by radial drainage, and the diameter of this circle is 3 times bigger than the stone column diameter. As mentioned in the results of numerical modelling, liquefaction for a depth of

Table 2. Parameters related to the stone column [17].

Characteristics	Permeability	Column Diameter	Friction Angle	Volumetric Modulus	Shear Modulus	Elasticity Modulus	Poisson's Ratio	Porosity
Unit	m/s	m	degree	MPa	MPa	MPa	-	-
Values	10^{-1}	0.9 1.2 ،1.5	48	50	23.1	60	0.3	0.3

Table 3. Summarizes the interface stiffness properties.

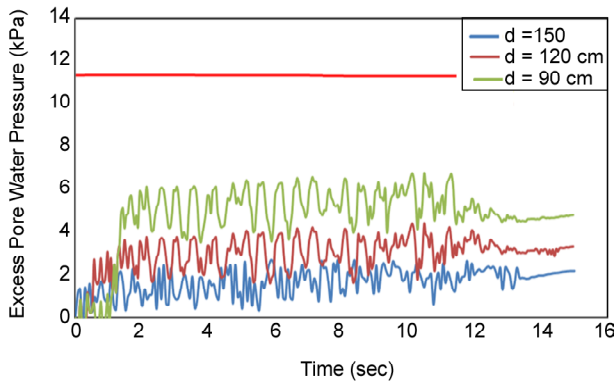| Characteristics	Normal Stiffness	Shear Stiffness	Friction Angle	Cohesion
Unit	MPa	MPa	Degree	MPa
Values	134	134	30	0

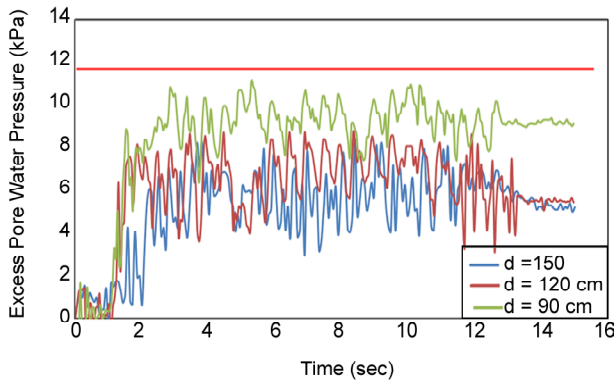**Figure 9.** The excess pore water pressure at 1 m.

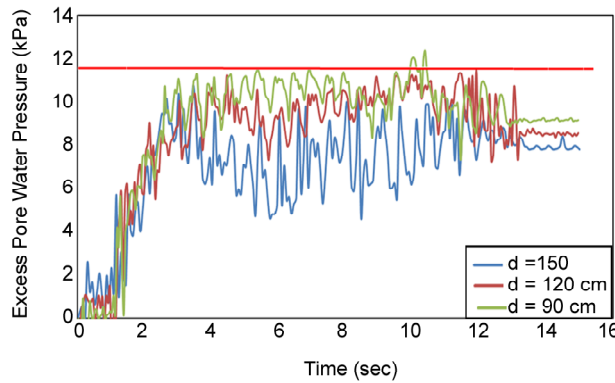**Figure 10.** The excess pore water pressure at 1.5 m.
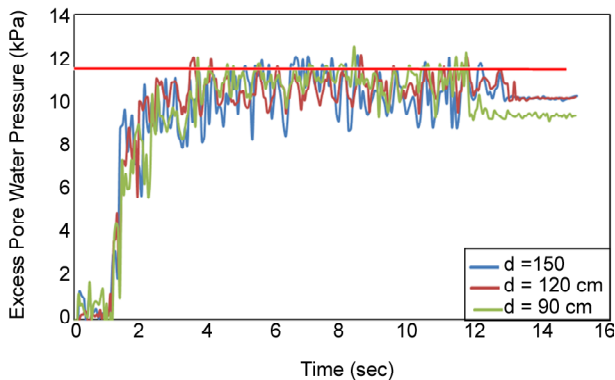

Figure 11. The excess pore water pressure at 2 m.

Figure 12. The excess pore water pressure at 2.5 m.

Table 4. The dynamic analysis results for 1.25 m depth.

Spacing (cm)	D = 150 cm	D = 120 cm	D = 90 cm
	r_u	r_u	r_u
Not Column	1	1	1
At 1 m	0.1	0.33	0.52
At 1.5 m	0.5	0.6	0.78
At 2 m	0.7	0.85	0.96
At 2.5 m	1	1	1

Table 5. The stone column performance for 1.25 m depth.

Performance	D = 150 cm	D = 120 cm	D = 90 cm
Diameter Area Improvement (cm)	430	380	270
Max Efficiency Liquefaction Risk Reduction	90%	67%	48%

1.25 m occurs in second 2 and r_u, but the effect of stone column in this depth and in the distance of 1 m from the center of column has decreased r_u to 0.1. Although liquefaction happens in farther distances from the stone column, the stone column delays the occurrence of liquefaction so that for the stone column with a diameter of 150 cm, the initial liquefaction in distance of 3 m from the column center occurs in the second 6 that is 4 seconds later than the case with no column. The best performance takes place in a column of a 150 cm diameter in 1 m from the center of a stone column so that the occurrence of liquefaction was decreased up to 90%.

The dynamic analysis results for 2.5 m depth of 1 m, 1.5 m, 2 m, 2.5 m and 3 m distances from the column's center are shown in Figures (13) to (17). Besides, the area of effective stress is equal to 23 kPa (red line) corresponding to static conditions in depth of 2.5 m.

Tables (6) and (7) shows the results of numerical modelling of the single stone column for a depth of 2.5 m. The results show that the circular region around the column is affected by radial drainage, and the diameter of this circle is four times bigger than the stone column diameter. The best perform-ance is for single column with a diameter of 150 cm in one meter from the center of a stone column so that the occurrence of liquefaction was decreased up to 92%. The results show that the performance of the column in depth of 2.5 m is better than that in depth of 1.25 m so that the primary liquefaction
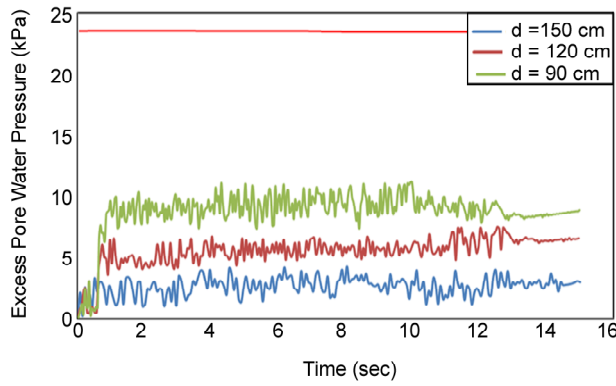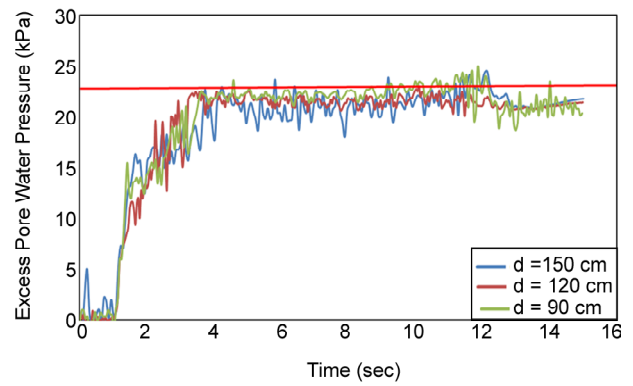
Figure 13. The excess pore water pressure at 1 m.
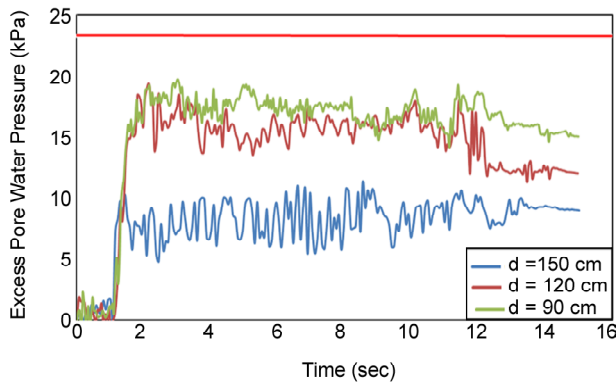

Figure 14. The excess pore water pressure at 1.5 m.

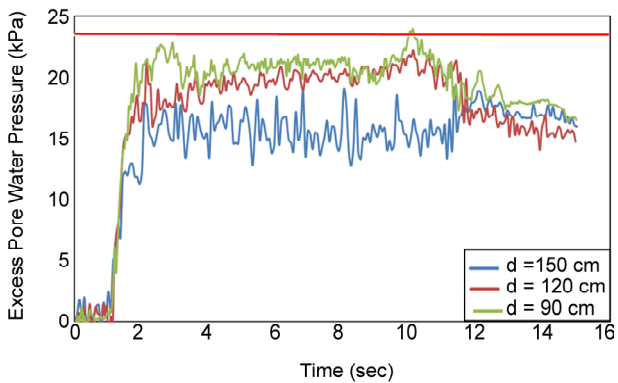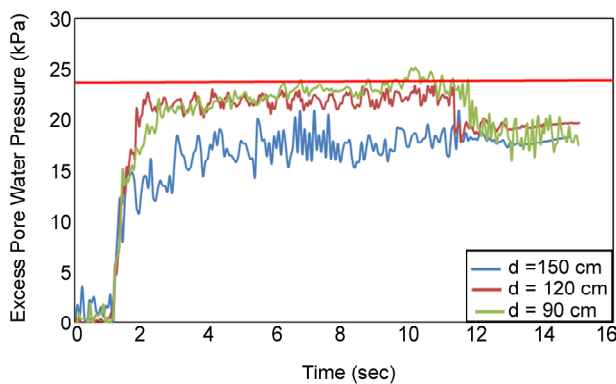**Figure 15.** The excess pore water pressure at 2 m.

Figure 16. The excess pore water pressure at 2.5 m.

Figure 17. The excess pore water pressure at 3 m.

Table 6. The dynamic analysis results for 2.5 m depth.

Spacing (cm)	D = 150 cm	D = 120 cm	D = 90 cm
	r_u	r_u	r_u
Not column	1	1	1
At 1 m	0.08	0. 3	0.43
At 1.5 m	0.34	0.68	0.77
At 2 m	0.78	0.86	0.96
At 2.5 m	0.84	1	1
At 3 m	1	1	1

Table 7. The stone column performance for 2.5 m depth.

Performance	D=150 cm	D=120 cm	D=90 cm
Diameter Area Improvement (cm)	580	450	360
Max Efficiency Liquefaction Risk Reduction	92%	70%	57%

does not occur in depth of 2.5m and a distance of 2.5 m from the center of a column with a diameter of 150 cm. Therefore, comparing the occurrence of liquefaction for depths of 1.25 m and 2.5 m shows that the performance of column increases with an increment of depth.

5. Numerical Modelling of Group Stone Columns

5.1. Model Geometry and Unit Cell Concept

Stone columns are commonly installed in square and triangle patterns, where in this study the square arrangement was used for stone column group modelling. For purposes of settlement and stability analyses, it is convenient to associate the tributary area of soil surrounding each stone column with the column as investigated. Although the tributary area forms a regular hexagon about the stone column, it can be closely approximated as an equivalent circle

having the same total area. For a square grid of stone columns, the equivalent circle has an effective diameter determined by the Eq. (5) [17]:

$$D_e = 1.13 \times S \tag{5}$$

where S is the spacing of stone columns. The resulting equivalent cylinder of material having a diameter D_e enclosing the tributary soil and one stone column is known as the unit cell. In this section of modelling, nine stone columns were placed together in a square arrangement, as shown in Figure (18). Considering the importance of columns' center-to-center distance in stone columns group behaviour, a sensitivity analysis was performed on column center-to-center distance to diameter ratio ($\frac{s}{d}$) in the current study. To do so, the above-mentioned ratio equal to 2, 3, 4 and 5 values was investigated in 90, 120 and 150 cm stone column diameters.

5.2. Area Replacement Ratio

The volume of soil replaced by stone columns has an important effect upon the performance of the improved ground. To quantify the amount of soil
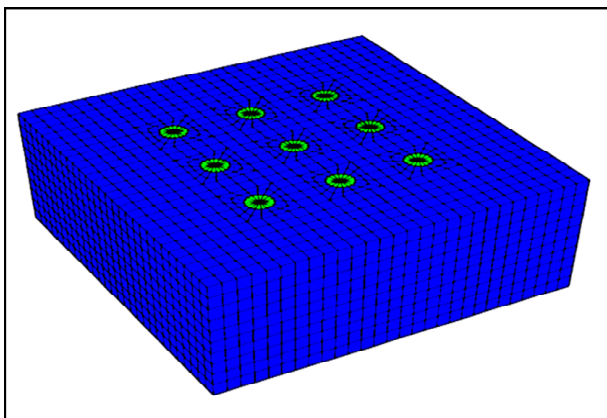
replacement, define the Area Replacement Ratio, or Improvement Factor as the fraction of a soil tributary to the stone column replaced by the stone and determined by the Eq. (6) [17]:

$$A_r = \frac{A_{SC}}{A_e} \tag{6}$$

where A_{SC} is the area of the stone column after compaction, and is the total area within the unit cell. Table (8) shows the details of area, replacement ratio and unit cell in group stone column.

5.3. Modifying the Soil Characteristics in Unit Cell

Baez [18] developed empirical relationships to estimate the expected improvement for a given pretreatment in terms of overburden corrected SPT/ CPT values. Figure (19) shows such a relationship graphically which is applicable fine to medium silty sand with fines less than 15% and little or no clay content. The replacement area ratio, A_r, is defined as the ratio of stone column area to the unit cell area per stone column in the previous section.

In order to determine the modified elasticity modulus in the unit cell, Eq. (7) was used, and Eq. (8) was applied for determining the soil's modified internal friction angle [20].

$$E_S = 500((N_1)_{60} + 15) \tag{7}$$

Figure 18. The finite difference mesh for group column with a diameter of 150 cm and 4.5 m center-to-center distance [13].
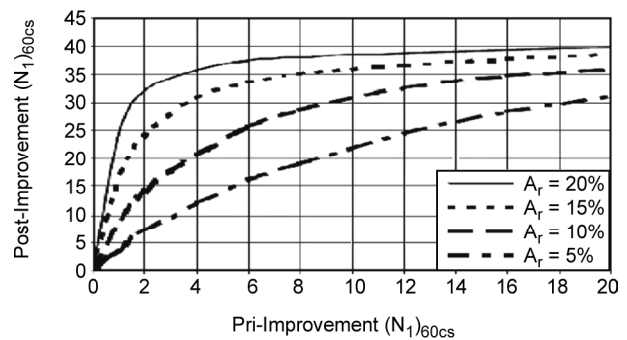
Figure 19. Prediction on Post-SPT based on Pre-SPT [19].

Table 8. The column spacing, unit cell and in pattern of square grid for various columns.

$\frac{s}{d}$	D = 150 cm			D = 120 cm			D = 90 cm		
	Spacing (cm)	Diameter of Unit Cell (cm)	A_r	Spacing (cm)	Diameter of Unit Cell (cm)	A_r	Spacing (cm)	Diameter of Unit Cell (cm)	A_r
2	300	339	20%	240	270	20%	180	203	20%
3	450	508	10%	360	406	10%	270	305	10%
4	600	678	5%	480	542	5%	360	406	5%
5	750	848	3%	600	675	3%	450	508	3%

$$\phi = 0.36(N_1)_{60} + 27 \qquad (8)$$

where in these equations, E_S is new elasticity modulus for the unit cell zone, ϕ is new friction angle for the unit cell zone, and $(N_1)_{60}$ is the new SPT number of unit cell. Using the pre-improvement SPT number and area, replacement ratio, A_r in the diagram in Figure (19) obtained E_S, $(N_1)_{60}$ and ϕ. For example, group stone column with 2.4 m center-to-center distance and square arrangement, $s/d = 2$ and diameter $=120$ cm, the following parameters can be considered:
$s/d=2$, and according to the diagram in Figure (19), we obtain $(N_1)_{60} = 37$, $E_S = 26 MPa$, $\phi = 40$.

5.4. Numerical Results of Group Stone Columns

The boundary conditions for static and dynamic analyses, the material models, wave transmission and dynamic loading condition in model of group stone column are similar to the single column analysis. The analysis results are presented in Figures (20) to (22) in terms of excess pore water pressure related to the middle point between the central column and the lateral column at 1.25 m depth for stone columns with diameter of 90, 120 and 150 cm.
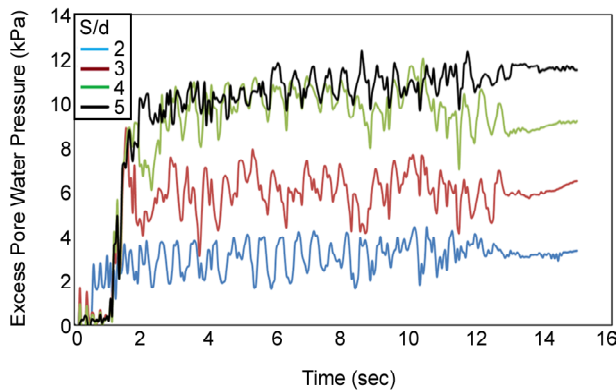
Table (9) shows the results of numerical modelling of the group stone column. The numerical modelling of group stone column with diameters of 90, 120, and 150 cm, according to the ratios of distances of columns from each other to their diameter ($s/d = 2, 3, 4, 5$) acts well to control liquefaction of excess pore water pressure. In the analysis, lateral columns help the central column in decreasing the pore water pressure and drainage. With, an increase in s/d ratio, the middle columns in groups act separately. Table (10) shows the columns performance in the group form. Table (11) shows the
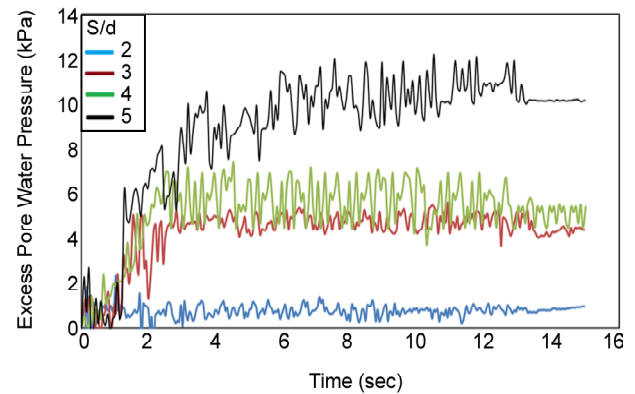

Figure 21. The excess pore water changes for group of stone columns with 150 cm diameter and s/d = 2 to 5.

Figure 20. The excess pore water changes for group of stone columns with 120 cm diameter and s/d = 2 to 5.
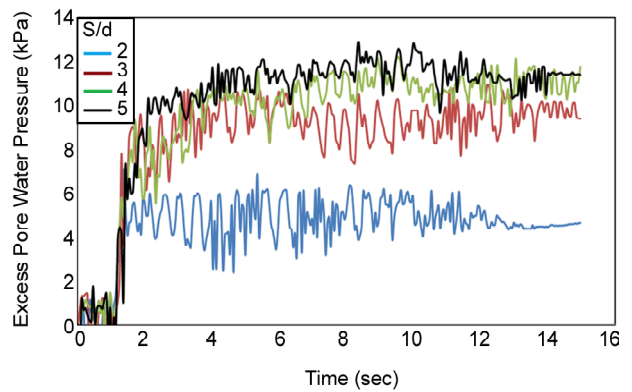
Figure 22. The excess pore water changes for group of stone columns with 90 cm diameter and s/d = 2 to 5.

Table 9. The result for group columns with 150, 120 and 90 cm diameter at 1.25 m depth.

s/d	D = 150 cm			D = 120 cm			D = 90 cm		
	r_u	Diameter of Improvement (cm)	Best Efficiency	r_u	Diameter of Improvement (cm)	Best Efficiency	r_u	Diameter of Improvement (cm)	Best Efficiency
2	0.08	300	92%	0.35	300	65%	0.5	180	50%
3	0.4	450	60%	0.6	400	40%	0.86	270	20%
4	0.86	500	45%	0.9	400	10%	1	270	0
5	1	600	0	1	400	0	1	270	0

Table 10. The group columns performance with 150, 120 and 90 cm diameter at 1.25 m depth.

s/d	D = 150 Performance	D = 120 Performance	D = 90 Performance
2	Group	Group	Group
3	Group	Group	Singular
4	Group	Singular	Singular
5	Singular	Singular	Singular

Table 11. Comparion for group columns and single column at 2 m distances from the center column at 1.25 m depth.

Performance	D = 150 cm		D = 120 cm		D = 90 cm	
	Diameter of Improvement (cm)	Max Efficiency Liquefaction Risk Reduction	Diameter of Improvement (cm)	Max Efficiency Liquefaction Risk Reduction	Diameter of Improvement (cm)	Max Efficiency Liquefaction Risk Reduction
Group	450	60%	400	40%	270	20%
Single	350	30%	300	15%	250	4%

Table 12. Ccomparison single performance in group form and single column at 3 m distances at 1.25 m depth .

Performance	D = 150 cm		D = 120 cm		D = 90 cm	
	Diameter of Improvement (cm)	Max Efficiency Liquefaction Risk Reduction	Diameter of Improvement (cm)	Max Efficiency Liquefaction Risk Reduction	Diameter of Improvement (cm)	Max Efficiency Liquefaction Risk Reduction
Group	500	45%	400	10%	270	0%
Single	350	0%	300	0%	250	0%

results of numerical modelling in the group performance and single performance for columns at 2 m distance from the center column. Table (12) shows the columns performance in the group form and then compare by single performance in group form at 3 m distance from the center column.

6. Conclusions

This paper studies the use of the stone columns as a means of mitigating earthquake-induced liquefaction in non-cohesive soils. The developed numerical model was validated on the basis of centrifuge test results from the model test No. 1 from well-known VELACS experimental project [2]. The liquefaction study was performed numerically using the finite difference computer code FLAC3D for NEVADA sand with 40% density. The results show that, the liquefaction in Finn Model [14] simulations are in good agreement with the VELACS experimental results [2]. Moreover, the effects of various parameters such as diameter of the stone columns, distance between columns on the liquefaction mitigating of NEVADA sand, soil, performance of the stone columns at different

depths of liquefiable soil, effective radius and effective depth were investigated. Then the effect of single stone column was investigated with different diameters on reduction of pore water pressure. Finally, the efficiency of group stone columns in square form was investigated by the simultaneous study of changes of diameter and distance in stone columns on excess pore water pressure dissipation. In general, the results show that the 3D model with a single stone column with diameter of 90, 120 and 150 cm acts well to control liquefaction. The results of numerical analyses show that the performance of the single stone column increases in reducing excess pore water pressure by increment of depth so that the stone column performance at 1.25 m depth with 150 cm diameter is a circular area with an approximate diameter of 430 cm, and the stone column performance at 2.5 m depth is an area with an approximate depth of 580 cm. Finally, it can be stated that at the depth of 1.25 m, the effective area of the column is three times bigger than the stone column diameter and for the depth of 2.5 m, this area is four times bigger than the stone column diameter.

The 3D numerical modelling from group stone columns with diameters of 90, 120 and 150 cm, according to the ratios of distances of columns from each other to their diameter (s/d = 2, 3, 4, 5) acts well to control liquefaction of excess pore water pressure. In the analysis, lateral columns helped the central column in decreasing the pore water pressure and drainage. With an increase in s/d ratio, the middle columns in groups act separately. The results show that, the group performance was dominant for s/d, and on the other hand, almost each column acts in a single manner for (s/d = 4, 5). Besides, the single manner in the group forms more effective than a single column. The group state's performance was better than the one of single column so that maximum efficiency in the liquefaction risk reduction is 92%. Moreover, the results show that the circular region around the stone column reduced excess pore water pressures smaller than the unit cell in group form.

References

1. Rayamajhi, D., Nguyen, T.V., Ashford, S.A., Boulanger, R.W., Lu, J., Elgamal, A., and Shao, L. (2012) Effect of discrete columns on shear stress distribution in liquefiable soil. *Proc., Geo-Congress 2012: State of the Art and Practice in Geotechnical Engineering*, ASCE, Reston, VA, 1908-1917.

2. Arulanandan, K. and Scott, R.F. (1993) Verification of numerical procedures for the analysis of soil liquefaction problems. *Proceeding of the International Conference on the Verification of Numerical Procedures for the Analysis of Soil Liquefaction Problems*, held at the University of California, Balkema Press, Rotterdam.

3. Mitchell, J.K. and Wentz, F.J. (1991) *Performance of Improved ground during the Loma Prieta Earthquake*.University of California, Berkeley, UCB/EERC Report 91/12, 26-37.

4. Adalier, K., Elgamal, A., Meneses, J., and Baez, I.J. (2003) Stone columns as liquefaction counter measure in non-plastic silty soils. *Journal of Soil Dynamics and Earthquake Engineering*, **23**(7), 571-584.

5. Brennan, A.J. and Madabhushi, S.P.G. (2002) Effectiveness of vertical drains in mitigation of liquefaction. *Soil Dynamics and Earthquake Engineering*, **22**(9-12), 1059-65.

6. Brennan, A.J. and Madabhushi, S.P.G. (2006) Liquefaction remediation by vertical drains with varying penetration depths. *Soil Dynamics and Earthquake Engineering*, **26**(5), 469-475.

7. Olgun, C.G. and Martin, J.R. (2008) Numerical modelling of the seismic response of Columnar reinforced ground. *Proc., Geotechnical Earthquake Engineering and Soil Dynamics IV*, ASCE, Reston, VA.

8. Bouckovalas, G.D., Papadimitriou, A.G., Kondis, A., and Bakas, G.J. (2006) Equivalent-uniform soil model for the seismic response analysis of sites improved with inclusions. *Proc., 6th European Conference on Numerical Methods in Geotechnical Engineering*, Taylor & Francis, London, 801-807.

9. Papadimitriou, A.G., Bouckovalas, G.D., Vytiniotis, A.C., and Bakas, G.J. (2006) Equivalence between 2D and 3D numerical simulations of the seismic response of improved sites. *Proc. 6th European Conference on Numerical Methods in Geotechnical Engineering*, Taylor & Francis, London, 809-815.

10. Asgari, A., Oliaei, M., Bagheri, M. (2013) Numerical simulation of improvement of a liquefiable soil layer using stone column and pile-pinning techniques. *Journal of Soil Dynamics and Earthquake Engineering*, (51), 77-96.

11. Brennan, A. and Papadimitriuo, A. (2007) Numerical Investigation of Liquefaction Mitigation Using Gravel Drains. *Proc. 14th Intl. Conf. Earthquake Engineering*, 15-48.

12. Arulmoli, K., Muraleetharan, K.K., Hossain, M.M., and Fruth, L.S. (1992) VELACS: Verification of liquefaction analysis of centrifuge studies, laboratory testing program, soil data report. *Earth Technology Corporation*, 51-58.

13. FLAC3D Version 3.0. Online Manual Table of Contents, Itasca 2005.

14. Finn, W.D.L., Lee, K.W., and Martin, G.R. (1997) An effective stress model for liquefaction.

Journal of Geotechnical Engineering Division, ASCE, **103**, 517-531.

15. Byrne, P. (1991) A cyclic shear-volume coupling and pore-pressure model for sand. *In Proc.: Second International Conference on Recent Advances in Geotechnical Earthquake Engineering and Soil Dynamics*, Paper No. 1.24, 47-55.

16. Baez, J.I. and Martin, G.R. (1993) Advances in the design of Vibro systems for the improvement of liquefaction resistance. *Proc. Symposium on Ground Improvement*, Vancouver Geotechnical Society, Vancouver, B.C., 62-70

17. FHWA (1983) *Design and Construction of Stone Column.* **I**, Report No. FHWA/RD-83/026.

18. Baez, J.I. (1995) *A Design Model for the Reduction of Soil Liquefaction by Vibro-Stone Columns*. Ph.D. Dissertation, USC, Los Angeles, CA. 207, 24-31.

19. Schaefer, V.R., Abramson, L.W., Drumheller, J.C., Hussin, J.D., and Sharp, K.D. (1997) *Ground Improvement Ground Reinforcement Ground Treatment: Developments 1987-1997*. Geotechnical Special Publication No. 69, ASCE, Logan, Utah, ISBN: 0784402604.

20. Bowles, J.E. (1996) *Foundation Analysis and Design*. McGraw-Hill, 5th Edition.